

# Shell-model calculations for neutron-rich carbon isotopes with a chiral nucleon-nucleon potential

L. Coraggio,<sup>1</sup> A. Covello,<sup>1,2</sup> A. Gargano,<sup>1</sup> and N. Itaco<sup>1,2</sup>

<sup>1</sup>*Istituto Nazionale di Fisica Nucleare,*

*Complesso Universitario di Monte S. Angelo, Via Cintia - I-80126 Napoli, Italy*

<sup>2</sup>*Dipartimento di Scienze Fisiche, Università di Napoli Federico II,*

*Complesso Universitario di Monte S. Angelo, Via Cintia - I-80126 Napoli, Italy*

(Dated: May 18, 2010)

We have studied neutron-rich carbon isotopes in terms of the shell model employing a realistic effective hamiltonian derived from the chiral  $N^3\text{LOW}$  nucleon-nucleon potential. The single-particle energies and effective two-body interaction have been both determined within the framework of the time-dependent degenerate linked-diagram perturbation theory. The calculated results are in very good agreement with the available experimental data, providing a sound description of this isotopic chain toward the neutron dripline. The correct location of the dripline is reproduced.

PACS numbers: 21.60.Cs, 23.20.Lv, 27.20.+n, 27.30.+t

The advances in the production of exotic beams are making possible the exploration of isotopes at and close to the neutron dripline. This is a major goal of nuclear physics, since these studies may reveal exotic features, such as shell modifications, that go beyond our present understanding of the structure of nuclei. In a recent Letter [1] Tanaka *et al.* have reported on the observation of a large reaction cross section in the dripline nucleus  $^{22}\text{C}$ . The structure of  $^{22}\text{C}$  is quite interesting, because it can be considered the heaviest Borromean nucleus ever observed [2]. This nucleus is weakly bound with a two-neutron separation energy  $S_{2n}$  evaluated to be  $420 \pm 940$  keV [1], and may be seen as composed of three parts: two neutrons plus  $^{20}\text{C}$ . These three pieces must all be present in order to obtain a bound  $^{22}\text{C}$  because of the particle instability of  $^{21}\text{C}$ . This is the structure of a Borromean nucleus, which has only one bound state but, considered as three-body system, admits no bound states in the binary subsystems [3].

The scope of the present work is to perform a theoretical study of the properties of heavy carbon isotopes approaching the neutron dripline. Our framework is the nuclear shell model, with both single-particle energies and residual two-body interaction derived directly from a realistic free nucleon-nucleon ( $NN$ ) potential. This fully microscopic approach to shell-model calculations, where no adjustable parameter is introduced, has already proved to be successful in reproducing the neutron dripline for the oxygen isotopes [4] as well as the spectroscopic properties of the  $p$ -shell nuclei [5] and  $N = 82$  isotones [6].

This is the first time that a realistic shell-model calculation is performed in this region. In fact, most of shell-model calculations to date have been performed employing empirical single-particle energies and two-body matrix elements adjusted to reproduce selected experimental data using the full  $psd$  model space (see for example [7, 8] and references therein).

We now give a short description of our calculations. We have carried out shell-model calculations, using the

Oslo shell-model code [9], for the heavy carbon isotopes in terms of valence neutrons occupying the three single-particle levels  $0d_{5/2}$ ,  $0d_{3/2}$ , and  $1s_{1/2}$ , with  $^{14}\text{C}$  considered as an inert core. This choice is mainly motivated by the observed large energy gap ( $\sim 6$  MeV) between the ground and first excited state. It is worth mentioning that in [10] it is suggested that the anomalous suppression of the observed  $B(E2; 2_1^+ \rightarrow 0_1^+)$  transition rates in  $^{14-18}\text{C}$  indicates a possible proton-shell closure in the neutron-rich carbon nuclei.

The shell-model effective hamiltonian  $H_{\text{eff}}$  has been derived within the framework of the time-dependent degenerate linked-diagram perturbation theory [11], starting from the  $N^3\text{LOW}$  nucleon-nucleon potential [4]. The latter is a low-momentum potential derived from chiral perturbation theory at next-to-next-to-next-to-leading order with a sharp momentum cutoff at  $2.1 \text{ fm}^{-1}$ . More explicitly, we have derived  $H_{\text{eff}}$  using the well-known  $\hat{Q}$ -box plus folded-diagram method [11], where the  $\hat{Q}$ -box is a collection of irreducible valence-linked Goldstone diagrams, which we have calculated through third order in the  $N^3\text{LOW}$  potential.

TABLE I: Theoretical shell-model single-particle energies (in MeV) employed in present work (see text for details).

$nlj$	Single-particle energies
$0d_{5/2}$	0.601
$0d_{3/2}$	5.121
$1s_{1/2}$	-0.793

The hamiltonian  $H_{\text{eff}}$  contains one-body contributions, whose collection is the so-called  $\hat{S}$ -box [12]. In realistic shell-model calculations it is customary to use a subtraction procedure, so that only the two-body terms of  $H_{\text{eff}}$ , which make up the effective interaction  $V_{\text{eff}}$ , are retained while the single-particle energies are taken from experiment. In this work, however, we have adopted a different approach employing single-particle energies obtained

from the  $\hat{S}$ -box calculation. In this connection, it is worth noting that the observed lowest  $J^\pi = \frac{1}{2}^+, \frac{5}{2}^+, \frac{3}{2}^+$  states in  $^{15}\text{C}$  are not pure single-particle states [13]. In Table I our calculated single-particle energies are reported. It should be noted that the experimental one-neutron separation energy of  $^{15}\text{C}$  ( $S_n=1.22$  MeV [14]) is slightly underestimated. For the sake of completeness, in Table ?? we also report the two-body matrix elements of  $V_{\text{eff}}$ .

TABLE II: Proton-proton, neutron-neutron, and proton-neutron matrix elements (in MeV). They are antisymmetrized, and normalized by a factor  $1/\sqrt{(1+\delta_{ja,jb})(1+\delta_{jc,jd})}$ .

$n_a l_a j_a$	$n_b l_b j_b$	$n_c l_c j_c$	$n_d l_d j_d$	$J$	$T_z$	TBME
$0p_{1/2}$	$0p_{1/2}$	$0p_{1/2}$	$0p_{1/2}$	0	1	-0.657
$0d_{5/2}$	$0d_{5/2}$	$0d_{5/2}$	$0d_{5/2}$	0	-1	-2.913
$0d_{5/2}$	$0d_{5/2}$	$0d_{3/2}$	$0d_{3/2}$	0	-1	-3.009
$0d_{5/2}$	$0d_{5/2}$	$1s_{1/2}$	$1s_{1/2}$	0	-1	-1.641
$0d_{3/2}$	$0d_{3/2}$	$0d_{3/2}$	$0d_{3/2}$	0	-1	-1.405
$0d_{3/2}$	$0d_{3/2}$	$1s_{1/2}$	$1s_{1/2}$	0	-1	-1.192
$1s_{1/2}$	$1s_{1/2}$	$1s_{1/2}$	$1s_{1/2}$	0	-1	-1.244
$0d_{5/2}$	$0d_{3/2}$	$0d_{5/2}$	$0d_{3/2}$	1	-1	-0.433
$0d_{5/2}$	$0d_{3/2}$	$0d_{3/2}$	$1s_{1/2}$	1	-1	-0.097
$0d_{3/2}$	$1s_{1/2}$	$0d_{3/2}$	$1s_{1/2}$	1	-1	0.178
$0d_{5/2}$	$0d_{5/2}$	$0d_{5/2}$	$0d_{5/2}$	2	-1	-1.102
$0d_{5/2}$	$0d_{5/2}$	$0d_{5/2}$	$0d_{3/2}$	2	-1	-0.073
$0d_{5/2}$	$0d_{5/2}$	$0d_{5/2}$	$1s_{1/2}$	2	-1	-0.990
$0d_{5/2}$	$0d_{5/2}$	$0d_{3/2}$	$0d_{3/2}$	2	-1	-0.804
$0d_{5/2}$	$0d_{5/2}$	$0d_{3/2}$	$1s_{1/2}$	2	-1	1.184
$0d_{5/2}$	$0d_{3/2}$	$0d_{5/2}$	$0d_{3/2}$	2	-1	-0.252
$0d_{5/2}$	$0d_{3/2}$	$0d_{5/2}$	$1s_{1/2}$	2	-1	-0.378
$0d_{5/2}$	$0d_{3/2}$	$0d_{3/2}$	$0d_{3/2}$	2	-1	-0.810
$0d_{5/2}$	$0d_{3/2}$	$0d_{3/2}$	$1s_{1/2}$	2	-1	0.893
$0d_{5/2}$	$1s_{1/2}$	$0d_{5/2}$	$1s_{1/2}$	2	-1	-1.317
$0d_{5/2}$	$1s_{1/2}$	$0d_{3/2}$	$0d_{3/2}$	2	-1	-0.847
$0d_{5/2}$	$1s_{1/2}$	$0d_{3/2}$	$1s_{1/2}$	2	-1	1.347
$0d_{3/2}$	$0d_{3/2}$	$0d_{3/2}$	$0d_{3/2}$	2	-1	0.121
$0d_{3/2}$	$0d_{3/2}$	$0d_{3/2}$	$1s_{1/2}$	2	-1	0.338
$0d_{3/2}$	$1s_{1/2}$	$0d_{3/2}$	$1s_{1/2}$	2	-1	-0.425
$0d_{5/2}$	$0d_{3/2}$	$0d_{5/2}$	$0d_{3/2}$	3	-1	0.594
$0d_{5/2}$	$0d_{3/2}$	$0d_{5/2}$	$1s_{1/2}$	3	-1	-0.099
$0d_{5/2}$	$1s_{1/2}$	$0d_{5/2}$	$1s_{1/2}$	3	-1	0.600
$0d_{5/2}$	$0d_{5/2}$	$0d_{5/2}$	$0d_{5/2}$	4	-1	-0.012
$0d_{5/2}$	$0d_{5/2}$	$0d_{5/2}$	$0d_{3/2}$	4	-1	-1.558
$0d_{5/2}$	$0d_{3/2}$	$0d_{5/2}$	$0d_{3/2}$	4	-1	-1.353
$0p_{1/2}$	$1s_{1/2}$	$0p_{1/2}$	$1s_{1/2}$	0	0	-1.752
$0p_{1/2}$	$0d_{3/2}$	$0p_{1/2}$	$0d_{3/2}$	1	0	-0.454
$0p_{1/2}$	$0d_{3/2}$	$0p_{1/2}$	$1s_{1/2}$	1	0	-0.024
$0p_{1/2}$	$1s_{1/2}$	$0p_{1/2}$	$1s_{1/2}$	1	0	-1.148
$0p_{1/2}$	$0d_{5/2}$	$0p_{1/2}$	$0d_{5/2}$	2	0	-2.358
$0p_{1/2}$	$0d_{5/2}$	$0p_{1/2}$	$0d_{3/2}$	2	0	-0.594
$0p_{1/2}$	$0d_{3/2}$	$0p_{1/2}$	$0d_{3/2}$	2	0	-1.560
$0p_{1/2}$	$0d_{5/2}$	$0p_{1/2}$	$0d_{5/2}$	3	0	-2.346

We have performed calculations for carbon isotopes with  $A$  ranging from 16 up to 24, i.e. for systems with valence neutrons from  $N_{\text{val}}=2$  up to 10. In Fig. 1 the calculated ground-state energies of even-mass isotopes (continuous black line) relative to  $^{14}\text{C}$  are compared with the experimental ones (continuous red line) [14]. The ex-

perimental behavior is well reproduced, in particular our results confirm that  $^{22}\text{C}$  is the last bound isotope; its calculated  $S_{2n}$  is 601 keV to be compared with the evaluation of 420 keV [14]. Moreover, our calculations predict that  $^{21}\text{C}$  is unstable against one-neutron decay, the theoretical  $S_n$  being -1.6 MeV. Therefore, our results fit the picture of  $^{22}\text{C}$  as a Borromean nucleus.

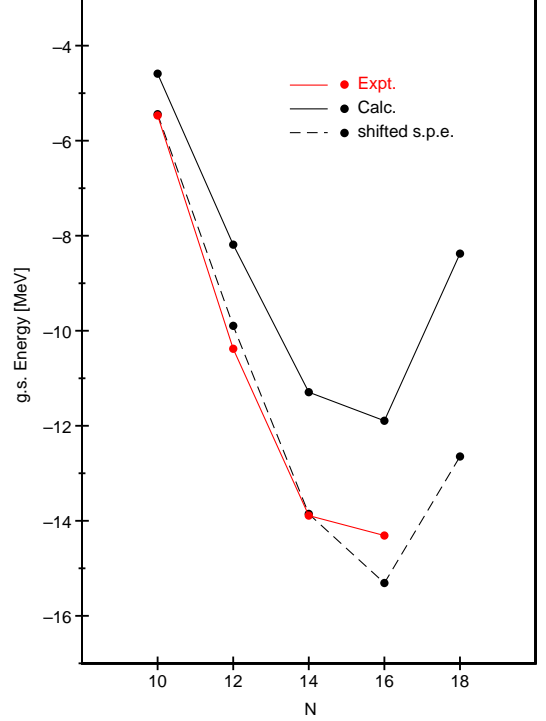


FIG. 1: (Color online) Experimental [1, 14] and calculated ground-state energies for carbon isotopes from  $A = 16$  to 24.  $N$  is the number of neutrons. See text for details.

From the inspection of Fig. 1, it can be seen that our calculations underestimate the experimental data. It is worth noting that this discrepancy may be “healed” by downshifting the single-particle spectrum so as to reproduce the experimental ground-state energy of  $^{15}\text{C}$  relative to  $^{14}\text{C}$ . The results obtained with this downshift (-427 keV) are reported in Fig. 1 by the black dashed line.

In Fig. 2, we report the experimental and calculated low-energy levels of the odd-mass nuclei  $^{17}\text{C}$  and  $^{19}\text{C}$ . It should be pointed out that the experimental levels shown in Fig. 2 are the only observed bound states. We see that the theory provides a satisfactory description of these states, apart from the inversion between the  $J^\pi = \frac{5}{2}^+$  and  $\frac{1}{2}^+$  states in  $^{17}\text{C}$ .

We have calculated the magnetic dipole moments of the  $J^\pi = (\frac{1}{2}^+)_1, (\frac{5}{2}^+)_1$  states in  $^{15}\text{C}$ , and  $J^\pi = (\frac{3}{2}^+)_1$  state in  $^{17}\text{C}$  using an effective operator obtained at third order in perturbation theory, consistently with the derivation of  $H_{\text{eff}}$ . We have obtained  $\mu(\frac{1}{2}^+)_1 = -1.920$  n.m.,  $\mu(\frac{5}{2}^+)_1 = -1.803$  n.m., and  $\mu(\frac{3}{2}^+)_1 = -0.807$

n.m., to be compared with the experimental values  $\pm 1.720 \pm 0.009$  [15] n.m.,  $\pm 1.758 \pm 0.030$  n.m. [16], and

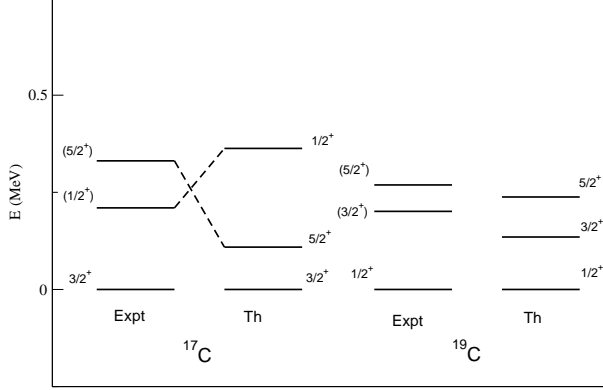


FIG. 2: Experimental [18] and calculated low-energy spectra for  $^{17}\text{C}$  and  $^{19}\text{C}$ .

Two magnetic dipole transition rates have been measured in  $^{17}\text{C}$ : the  $B(M1; \frac{1}{2}^+ \rightarrow \frac{3}{2}^+)$  and  $B(M1; \frac{5}{2}^+ \rightarrow \frac{3}{2}^+)$ . Our calculated values are respectively  $0.0941 \mu_N^2$  and  $0.095 \mu_N^2$ , to be compared with the experimental values of  $(0.0010 \pm 0.0001) \mu_N^2$  and  $(0.082^{+0.032}_{-0.018}) \mu_N^2$  [19]. It is worth mentioning that the anomalous quenching of the strength observed in the  $\frac{1}{2}^+ \rightarrow \frac{3}{2}^+$  transition has been recently reproduced in Ref. [7] in the framework of a shell-model calculation modifying the tensor components and the  $T = 1$  monopole terms of the empirical effective Hamiltonian *SFO* [20] defined in the the full *psd* model space.

TABLE III: Effective reduced single-neutron matrix elements of the magnetic dipole operator  $M1$  (in n.m.).

$n_a l_a j_a$	$n_b l_b j_b$	$\langle a    M1    b \rangle$
$0d_{5/2}$	$0d_{5/2}$	-2.553
$0d_{5/2}$	$0d_{3/2}$	2.743
$0d_{3/2}$	$0d_{5/2}$	-2.743
$0d_{3/2}$	$0d_{3/2}$	1.414
$0d_{3/2}$	$1s_{1/2}$	0.179
$1s_{1/2}$	$0d_{3/2}$	-0.179
$1s_{1/2}$	$1s_{1/2}$	-2.298

In Tables III we report the effective reduced single-neutron matrix elements of the  $M1$  operator.

In Fig. 3 we report the experimental excitation energies of the yrast  $2^+$  states as a function of  $A$  and compare them with our calculated values. It can be seen that the observed energies are reproduced nicely. We also report our predicted excitation energy, 4.661 MeV, for the unbound  $J^\pi = 2^+$  state in  $^{22}\text{C}$ .

TABLE IV: Effective reduced single-neutron matrix elements of the electric quadrupole operator  $E2$  (in  $e \text{ fm}^2$ ).

$n_a l_a j_a$	$n_b l_b j_b$	$\langle a    E2    b \rangle$
$0d_{5/2}$	$0d_{5/2}$	-3.357
$0d_{5/2}$	$0d_{3/2}$	-1.866
$0d_{5/2}$	$1s_{1/2}$	-1.826
$0d_{3/2}$	$0d_{5/2}$	1.866
$0d_{3/2}$	$0d_{3/2}$	-2.803
$0d_{3/2}$	$1s_{1/2}$	1.434
$1s_{1/2}$	$0d_{5/2}$	-1.826
$1s_{1/2}$	$0d_{3/2}$	-1.434

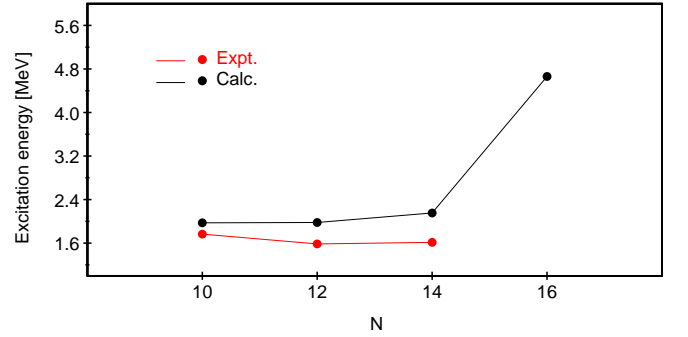


FIG. 3: (Color online) Experimental [21, 22] and calculated excitation energies of the yrast  $J^\pi = 2^+$  states for carbon isotopes from  $A = 16$  to  $22$ .  $N$  is the number of neutrons.

The behavior of the theoretical  $2^+$  excitation energies confirms that there is no  $N = 14$  subshell closure. We obtain a ground-state wave function in  $^{20}\text{C}$  with only 14% of the  $(\nu d_{5/2})^6$  configuration (calculated using the OXBASH shell-model code [23]). This is a direct consequence of the fact that the effective single-particle energy [24] of the  $1s_{1/2}$  state is the lowest one all along the carbon isotopic chain, as can be seen in Fig. 4. One can infer that the large energy gap between the  $0d_{3/2}$  level and the  $0d_{5/2}$ ,  $1s_{1/2}$  levels is responsible for the  $N = 16$  subshell closure.

It is worth mentioning that the behavior of the yrast  $2^+$  state in C isotopes is quite different from that shown by O isotopes, where a  $N = 14$  subshell closure has been evidenced. This is clearly related to the removal of the two protons from the  $0p_{1/2}$  level, which, in the case of oxygen isotopes, interact with the *sd* neutrons giving rise to a downshift of the  $0d_{5/2}$  neutron level relative to the  $1s_{1/2}$  one [8]. In this connection, we have verified that, using our effective hamiltonian, the effective single particle energy of the  $0d_{5/2}$  state in  $^{17}\text{O}$  is lowered by 2.1 MeV relative to that of the  $1s_{1/2}$  one.

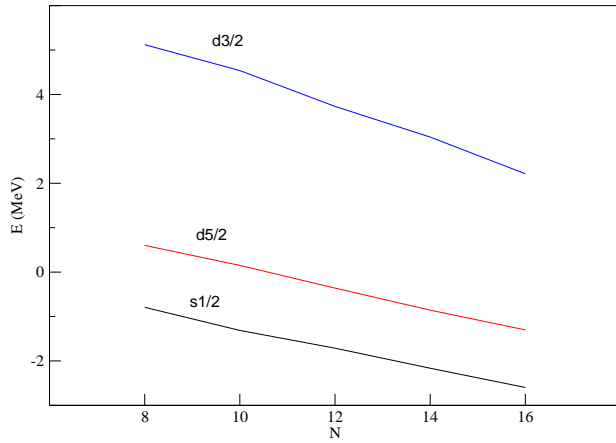


FIG. 4: (Color online) Effective single-particle energies of the neutron  $1s_{1/2}$ ,  $0d_{5/2}$ , and  $0d_{3/2}$  orbits from  $A = 16$  to 22.  $N$  is the number of neutrons.

We have calculated the  $B(E2; 2_1^+ \rightarrow 0_1^+)$  transition rates up to  $^{20}\text{C}$  employing the effective operator of Table IV. Our results are compared with the experimental data in Table V. We see that the agreement is quite good, providing evidence for the reliability of our calculated effective operator which takes into account microscopically core-polarization effects up to third order in the  $NN$  potential. It is well known [10, 21, 22, 25] that these observed transition strengths are strongly hindered when compared with the values obtained by an empirical formula based on the liquid-drop model [26]. In this connection, we would like to point out that our effective reduced single-neutron matrix elements (see Table IV)

correspond to a neutron effective charge of about 0.4e with an harmonic-oscillator parameter  $b = 1.72$  fm.

TABLE V: Experimental and calculated reduced transition probabilities  $B(E2; 2_1^+ \rightarrow 0_1^+)$  (in  $\text{e}^2\text{fm}^4$ ). Superscripts  $a$ ,  $b$ ,  $c$  refer to [10], [25], and [22], respectively. The experimental errors reported are the statistical and systematic ones, respectively.

Nucleus	Calc.	Expt.
$^{16}\text{C}$	1.8	$2.6 \pm 0.2 \pm 0.7^a$
$^{18}\text{C}$	3.0	$4.15 \pm 0.73^b$
$^{20}\text{C}$	3.7	$4.3 \pm 0.2 \pm 1.0^a$
		$< 3.7^c$

In summary, we have given here a shell-model description of heavy carbon isotopes, using a fully microscopic approach. This has been done by deriving from the realistic chiral  $NN$  potential  $\text{N}^3\text{LOW}$  both the single-particle energies and residual two-body interaction of the effective shell-model hamiltonian. Our calculations have led to a sound description of these isotopes when approaching the neutron dripline. As a matter of fact, they confirm the disappearance of the  $N = 14$  subshell closure that is present in the oxygen chain, and predict the  $N = 16$  one. In particular, we reproduce successfully the fact that  $^{22}\text{C}$  is the last bound isotope. It is worth mentioning that this nucleus, which has only recently been observed [1], is one of the most exotic of the 3000 known isotopes, its  $N/Z$  ratio being 2.67. The quality of the results obtained makes us confident that our approach may be a valuable tool to study nuclei far from the valley of stability.

- 
- [1] K. Tanaka, T. Yamaguchi, T. Suzuki, T. Ohtsubo, M. Fukuda, D. Nishimura, M. Takechi, K. Ogata, A. Ozawa, T. Izumikawa, et al., Phys. Rev. Lett. **104**, 062701 (2010).
  - [2] K. W. Kemper and P. D. Cottle, Physics **3**, 13 (2010).
  - [3] M. V. Zhukov, B. V. Danilin, D. V. Fedorov, J. M. Bang, I. J. Thompson, and J. S. Vaagen, Phys. Rep. **231**, 151 (1993).
  - [4] L. Coraggio, A. Covello, A. Gargano, N. Itaco, T. T. S. Kuo, D. R. Entem, and R. Machleidt, Phys. Rev. C **75**, 024311 (2007).
  - [5] L. Coraggio and N. Itaco, Phys. Lett. B **616**, 43 (2005).
  - [6] L. Coraggio, A. Covello, A. Gargano, N. Itaco, and T. T. S. Kuo, Phys. Rev. C **80**, 044320 (2009).
  - [7] T. Suzuki and T. Otsuka, Phys. Rev. C **78**, 061301(R) (2008).
  - [8] M. Stanoiu, D. Sohler, O. Sorlin, F. Azaiez, Z. Dombrádi, B. A. Brown, M. Bellegruic, C. Borcea, C. Bourgeois, Z. Dlouhy, et al., Phys. Rev. C **78**, 034315 (2008).
  - [9] T. Engeland, the Oslo shell-model code 1991-2006, unpublished.
  - [10] H. J. Ong, N. Imai, D. Suzuki, H. Iwasaki, H. Sakurai, T. K. Onishi, M. K. Suzuki, S. Ota, S. Takeuchi, T. Nakao, et al., Eur. Phys. J. A **42**, 393 (2009).
  - [11] L. Coraggio, A. Covello, A. Gargano, N. Itaco, and T. T. S. Kuo, Prog. Part. Nucl. Phys. **62**, 135 (2009).
  - [12] J. Shurpin, T. T. S. Kuo, and D. Strottman, Nucl. Phys. A **408**, 310 (1983).
  - [13] F. Ajzenberg-Selove, Nucl. Phys. A **523**, 1 (1991).
  - [14] G. Audi, A. H. Wapstra, and C. Thibault, Nucl. Phys. A **729**, 337 (2003).
  - [15] K. Asahi, K. Sakai, H. Ogawa, H. Miyoshi, K. Yogo, A. Goto, T. Suga, H. Ueno, Y. Kobayashi, A. Yoshimi, et al., Nucl. Phys. A **704**, 88c (2002).
  - [16] J. Asher, D. W. Bennett, B. A. Brown, H. A. Doubt, and M. A. Grace, J. Phys. G **6**, 251 (1980).
  - [17] H. Ogawa, K. Asahi, H. Ueno, K. Sakai, H. Miyoshi, D. Kameda, T. Suzuki, H. Izumi, N. Imai, Y. X. Watanabe, et al., Eur. Phys. J. A **13**, 81 (2002).
  - [18] Z. Elekes, Z. Dombrádi, R. Kanungo, H. Baba, Z. Fülöp, J. Gibelin, Á. Horváth, E. Ideguchi, Y. Ichikawa, N. Iwasa, et al., Phys. Lett. B **614**, 174 (2005).
  - [19] D. Suzuki, H. Iwasaki, H. J. Ong, N. Imai, H. Sakurai, T. Nakao, N. Aoi, H. Baba, S. Bishop, Y. Ichikawa, et al., Phys. Lett. B **666**, 222 (2008).
  - [20] T. Suzuki, R. Fujimoto, and T. Otsuka, Phys. Rev. C **67**, 044302 (2003).

- [21] H. J. Ong, N. Imai, D. Suzuki, H. Iwasaki, H. Sakurai, T. K. Onishi, M. K. Suzuki, S. Ota, S. Takeuchi, T. Nakao, et al., *Phys. Rev. C* **78**, 014308 (2008).
- [22] Z. Elekes, Z. Dombrádi, T. Aiba, N. Aoi, H. Baba, D. Bemmerer, B. A. Brown, T. Furumoto, Z. Fülöp, N. Iwasa, et al., *Phys. Rev. C* **79**, 011302 (2009).
- [23] B. A. Brown, A. Etchegoyen, and W. D. M. Rae, the Computer Code OXBASH, MSU-NSCL Report No. 524.
- [24] Y. Utsuno, T. Otsuka, T. Mizusaki, and M. Honma, *Phys. Rev. C* **60**, 054315 (1999).
- [25] M. Wiedeking, P. Fallon, A. O. Macchiavelli, J. Gibelin, M. S. Basunia, R. M. Clark, M. Cromaz, M.-A. Deleplanque, S. Gros, H. B. Jeppesen, et al., *Phys. Rev. Lett.* **100**, 152501 (2008).
- [26] S. Raman, C. W. Nestor, and K. H. Bhatt, *Phys. Rev. C* **37**, 805 (1988).